

Theory & Apparatus: NPOI

Or

*“How the NPOI is built and why”*

Don Hutter

May 24, 2001



## **Outline:**

- General considerations
- Array layout
- Siderostats, angle tracking & metrology
- Vacuum feed system
- Delay lines
- Beam combiners
- Fringe detection
- Automation

## **Programmatics:**

- *Funding:* Oceanographer of the Navy & Office of Naval Research (ONR)
- *Collaboration:* USNO & NRL, in cooperation with Lowell Observatory
- *Result* of efforts of ~77 people (currently 30, including shop)
- *Lowell:* site infrastructure development, maintenance & operations
- *USNO Instrument Shop:* nearly all precision mechanical fabrication
- *Contractors:* Interferometrics, USRA, Applied Research, SFA

## **Project History:**

Jul 1989	Design work commences
Sep 1991	Contract signed with Lowell Observatory
Sep 1992	Construction begins on Anderson Mesa
Jul 1993	Start installation of instrumentation
Oct 1994	First single-baseline observations
Mar 1996	Three baselines, first closure-phase data
May 1996	First binary star images (Mizar A)
Nov 1996	First limb-darkening observations
Sep 1997	Array metrology at three astrometric stations
Jun 1998	First two imaging siderostats operational
June 2000	6 <sup>th</sup> delay line, upgrades to beam combiner
May 2001?	First 6-way fringe detection

## Scientific Results:

- Approximately 27 publications to date (8 in referred journals) related to scientific results from NPOI observations:
  - **Stellar diameters** (50 stars; Nordgren *et al.* 1999, AJ, 118, 3032)
  - **Diameters of Cepheids** ( $\delta$  Cep,  $\eta$  Aql,  $\zeta$  Gem, Polaris)  
(Armstrong *et al.* 2001, AJ, 121, 476; Nordgren *et al.* 2000, ApJ, 543, 972)
  - **Binary orbits** ( $\zeta^1$  UMa,  $\eta$  Peg, o Leo,  $\zeta$  Ori,  $\phi$  Her)  
(Hummel *et al.* 2001, ApJ, in press; Hummel *et al.* 2000, ApJ Lett, 540, L91; Hummel *et al.* 1998, AJ, 116, 2536)
  - **Imaging** ( $\zeta^1$  UMa; Benson *et al.* 1997, AJ, 114, 1221)
  - **Limb darkening** ( $\alpha$  Cas,  $\alpha$  Ari; Hajian *et al.* 1998, ApJ, 496, 484)

## Basic Design Parameters:

Location:	Lowell Observatory, Anderson Mesa, AZ longitude = W111° 32' 2" latitude = N35° 5' 45" altitude = 2200 m (7220 ft)
Baseline lengths:	2.0 – 437 m (imaging sub-array) 19 – 38 m (astrometric sub-array)
Number of elements:	6 (imaging sub-array, movable) 4 (astrometric sub-array, fixed)
Aperture size:	12 cm (current, both sub-arrays) 35 cm (astrometric sub-array, 2002)
Bandpass:	450 – 850 nm 32 spectral channels
Features:	Vacuum feed and delay systems Active group-delay fringe tracking Array metrology (astrometric sub-array) Extensive automation

## Array Layout (Imaging):

- 6 movable siderostats, 30 stations:
- baselines 2 – 437 m
  - maximum resolution:
    - \* diameters:  $200\mu\text{as}$  @ 1% accuracy
    - \* binaries:  $65\mu\text{as}$  ( $\Delta m \sim 0$ ),  $200\mu\text{as}$  ( $\Delta m \sim 3-4$ )
- 6 elements: *compromise* b/w desire for more elements (better u,v coverage) and sensitivity (lower S/N when more beams combined), but also **COST!**



- number of equally spaced configurations (scaling  $\sim 1.65$ ) *"Semi-Redundant"*
  - optimal for imaging stellar surfaces:
    - \* must stabilize (track) fringes on star itself (small optical  $t_0$ )
    - \* stars are disk-like  $\Rightarrow V^2$  high only at low spatial freq, but info on limb darkening & surface structure only at high spatial frequencies where  $V^2$  very low
  - "phase bootstrapping" (baseline bootstrapping)
    - \* stabilize fringes on longest baselines by tracking on shortest baselines
  - improve  $u, v$  coverage by:
    - \* 2-D, Y-array (& switching elements b/w arms)
    - \* wide bandwidth

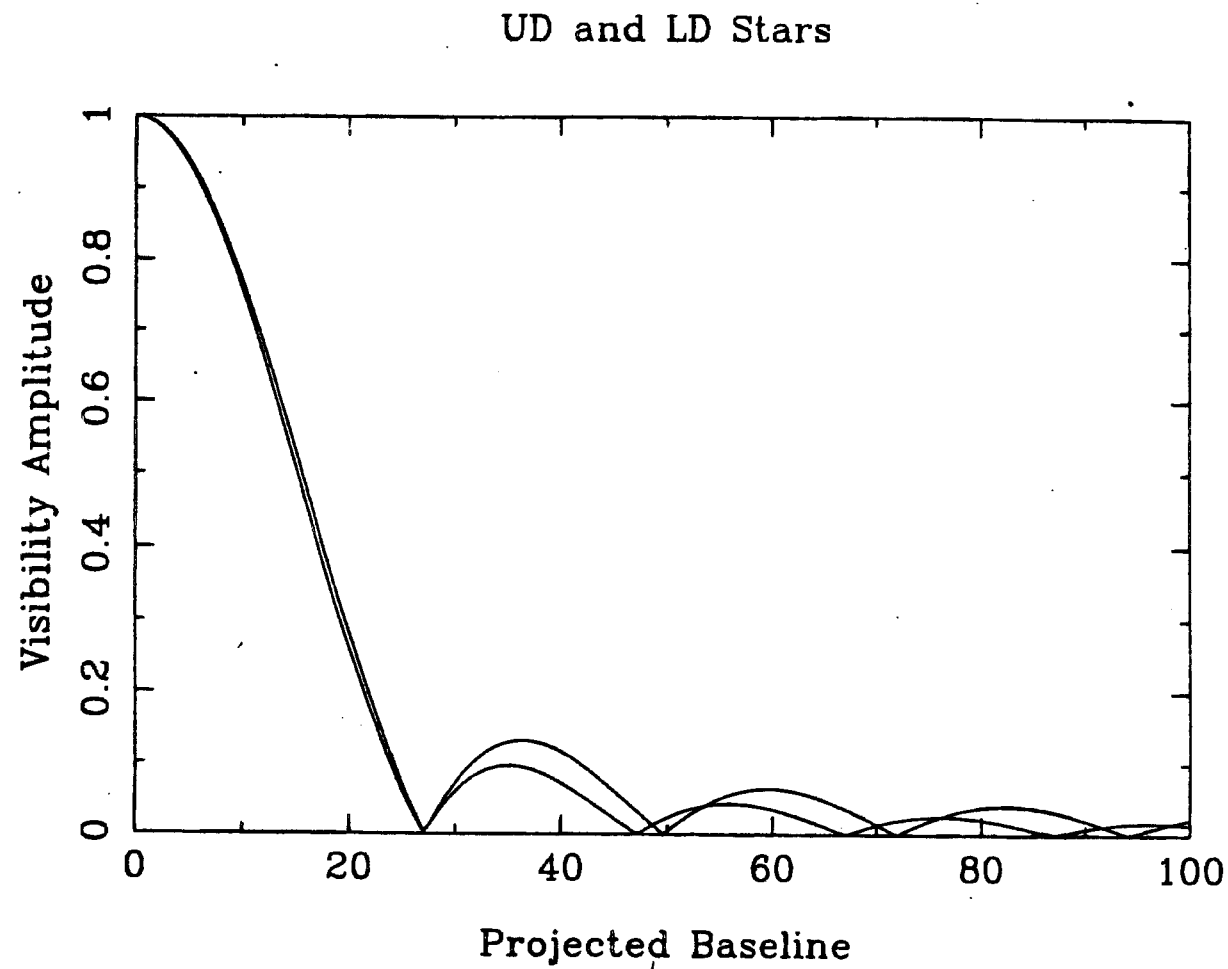


Figure 14.1: Visibility amplitude as a function of projected baseline for uniform and limb-darkened stars.

*MOZURKEWICH (Ref. 4)*

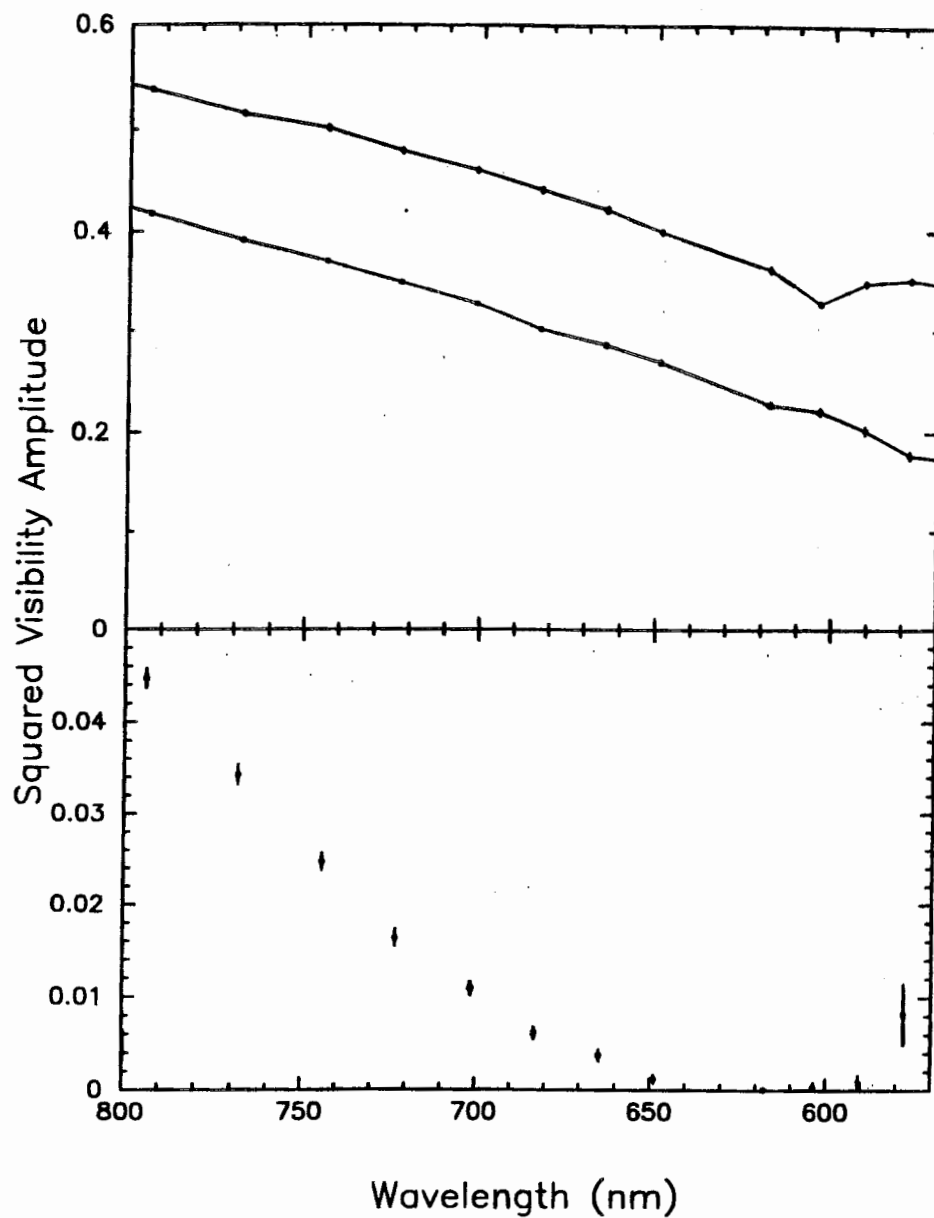
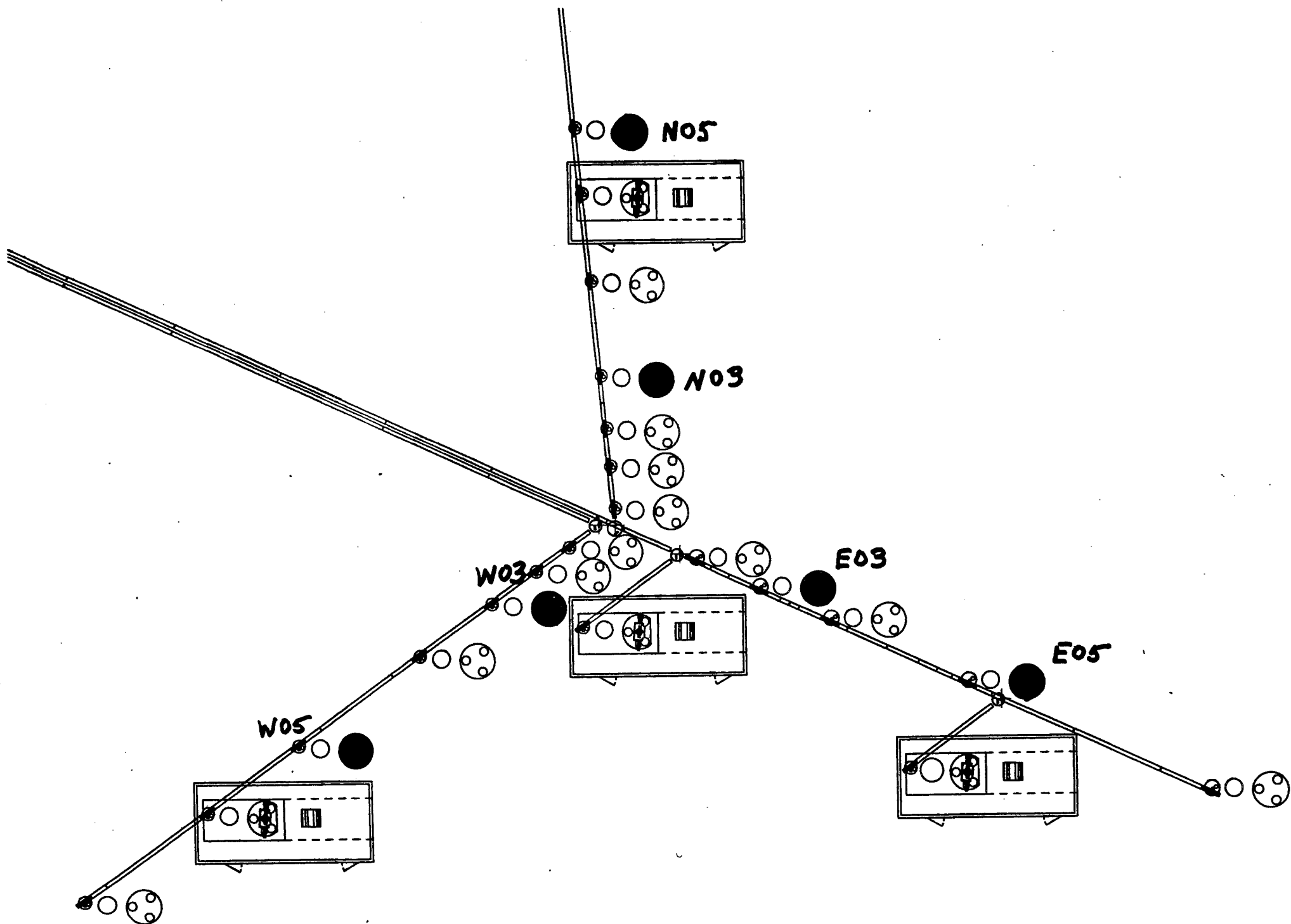


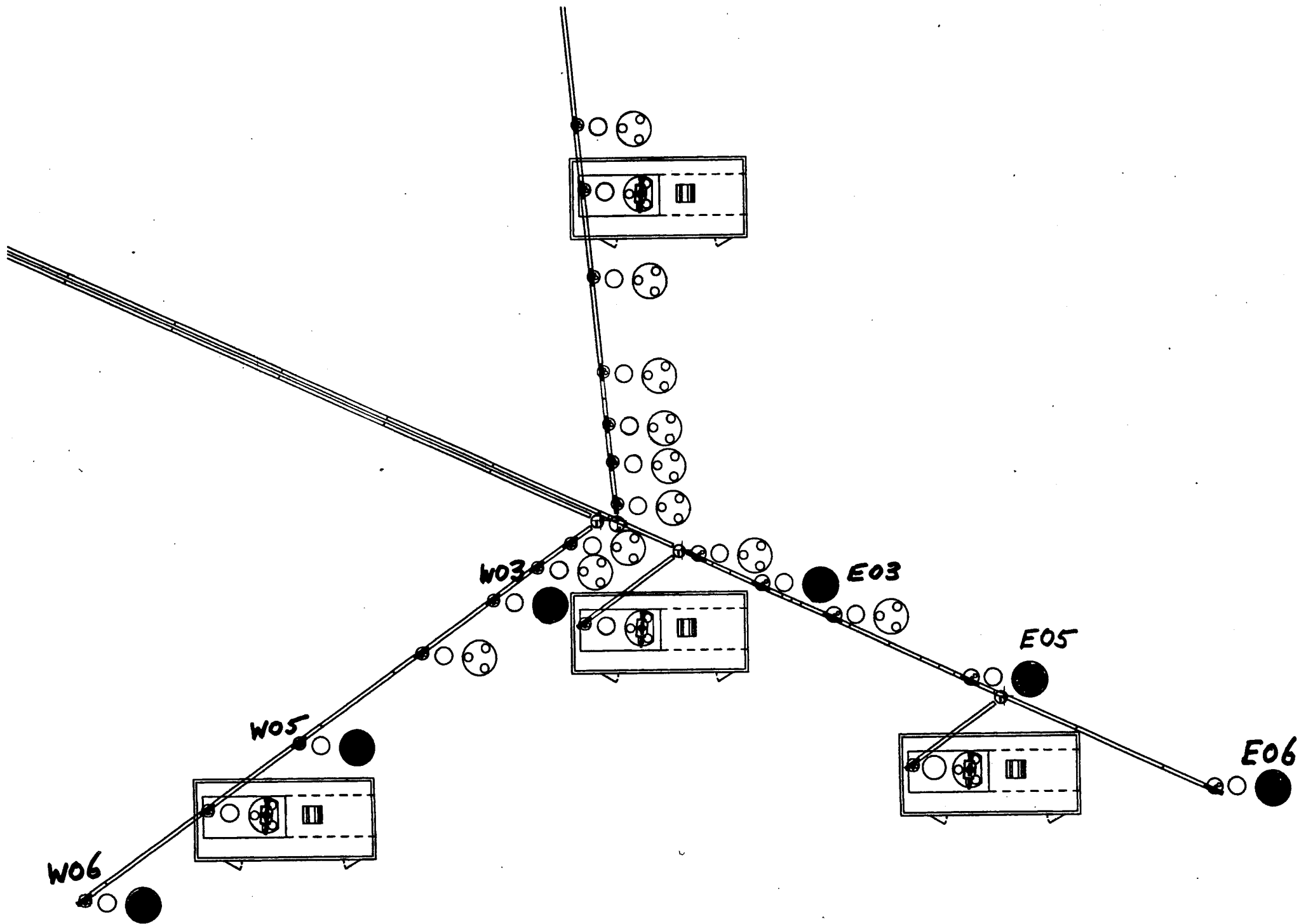
Figure 14.7: Fringe data as a function of wavelength from the NPOI. The data was taken simultaneously on all three baselines. The longest baseline (lower curve) was only obtained because the fringes were stabilized on that baseline using the two shorter baselines (upper curves).

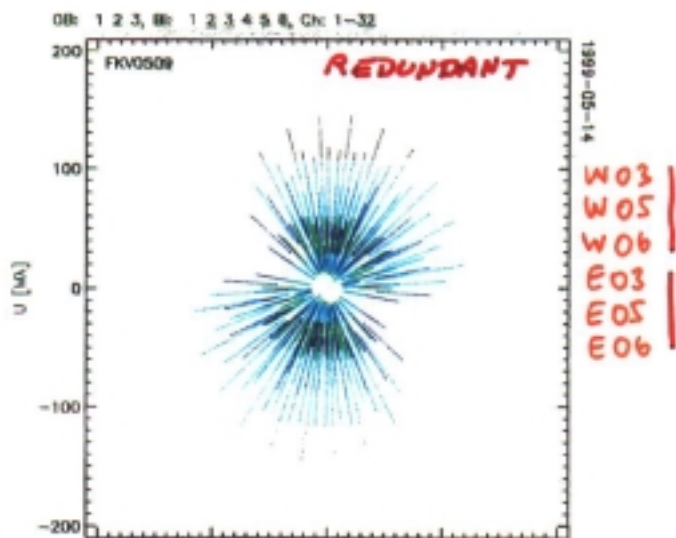
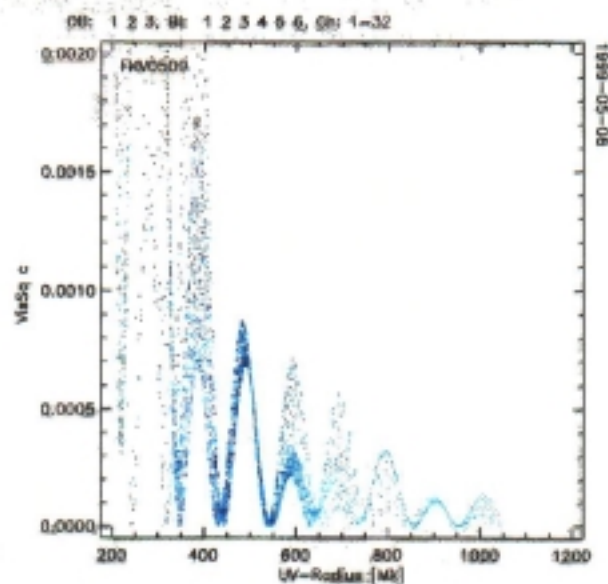
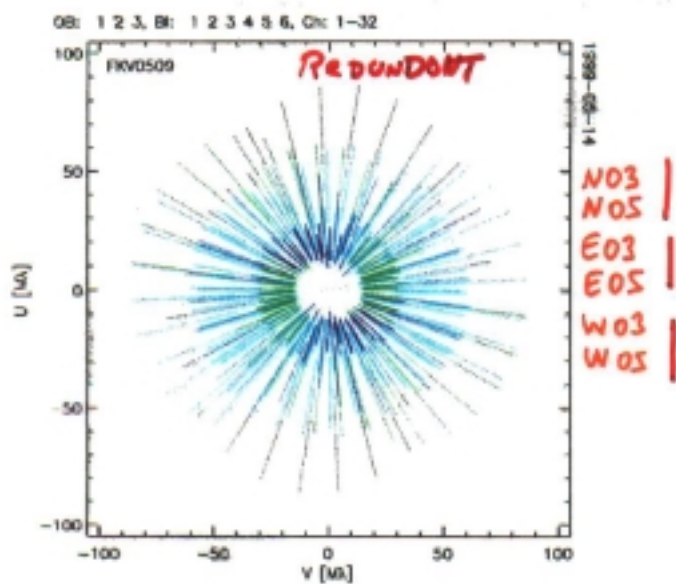
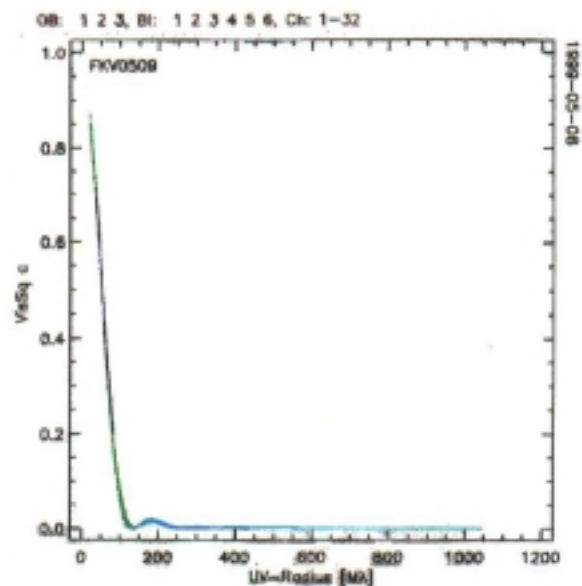
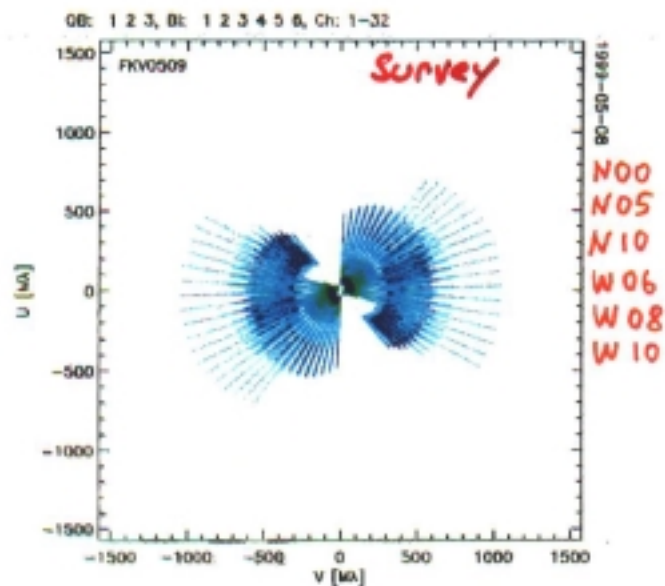
# Positions of imaging stations along arms of Y

Station number	Distance along arm (m)			Equally spaced configuration membership
	North arm	East arm	West arm	
00	0.53	...	...	...
01	2.75	...	2.87	A
02	4.76	4.78	5.05	B
03	7.55	8.55	7.98	A C
04	12.5	12.6	12.7	AB D
05	20.6	20.6	20.7	BC E
06	34.5	34.5	34.6	CD F
07	56.3	56.3	56.2	DE G
08	93.8	94.0	92.4	EF H
09	153.9	153.9	150.8	FG I
10	251.7	252.7	245.4	GH J

ARMSTRONG et al. (Ref 1)







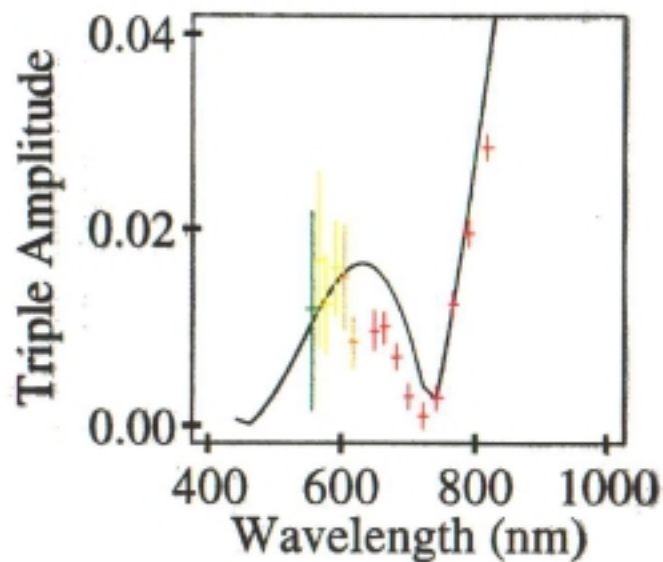
Uniform Disk



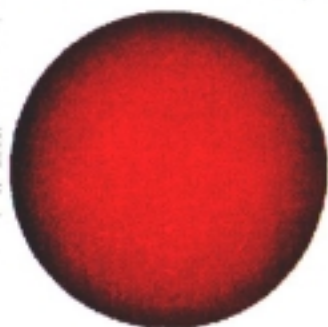
5.24 mas



$\alpha$  Cas - Dec 18, 1996.



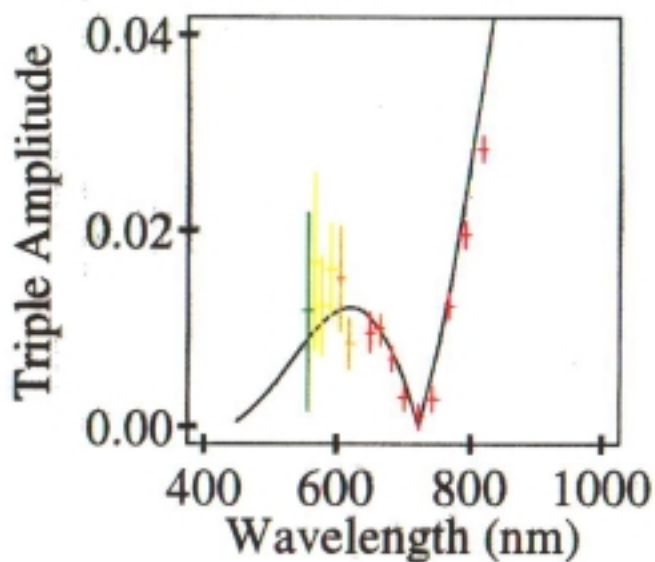
Limb-Darkened Disk



5.58 mas



$\alpha$  Cas - Dec 18, 1996.





- unequally spaced (optimal  $u, v$ ) arrays also available:
  - for surveys for duplicity & diameter
  - for imaging extended sources where sufficiently small, bright source is available to act as phase reference (unresolved on longest baseline)
    - \* circumstellar, circumbinary material
    - \* small & large star in binary
    - \* flare on surface of large star

### **Array Layout (Astrometry):**

- 4 fixed siderostats, baselines 19 – 38 m
- baseline length: compromise b/w positional resolution & resolving bright stars
  - 100 nm metrology on 20 m baseline for 1 mas astrometry
  - $V^2 > \text{few \%}$  for stars  $< 8 \text{ mas}$ )
- 4 elements:
  - allows simultaneous solution for stellar positions & baselines with as few as 11 stars observed only once ( $< 1 \text{ hour}$  observing)

## **Siderostats, Angle Tracking & Metrology:**

- Siderostats:
  - 50 cm clear-aperture flat in precision alt-az mount (built at USNO)
  - stepper motor drive w/planetary gear reduction  $\Rightarrow 10^8$  steps/rev
- Beam Compressors (astrometric stations only):
  - 35 cm aperture, off-axis optics
  - use (with good seeing) to measure positions of radio stars (link to radio frame)
- Wide-angle Star Acquisition (WASA) system: (30' FoV, 5" pixels):
  - frames analyzed to locate source & calculate siderostat point corrections
  - necessary to pass stellar beam to lab ( few arcsec FoV set by feed pipes)

- Narrow-angle Tracker (NAT):

- correct for image motion to superimpose beams at  $\sim 0.3$  arc sec rms (1% visibility loss)
- quad cell of APDs on beam combiner table measure image motion
- 20 cm tip-tilt mirror mounts (near siderostats) driven by piezos
- currently, servo closed at  $\sim 30$ Hz, prototype of stiffer mount under test

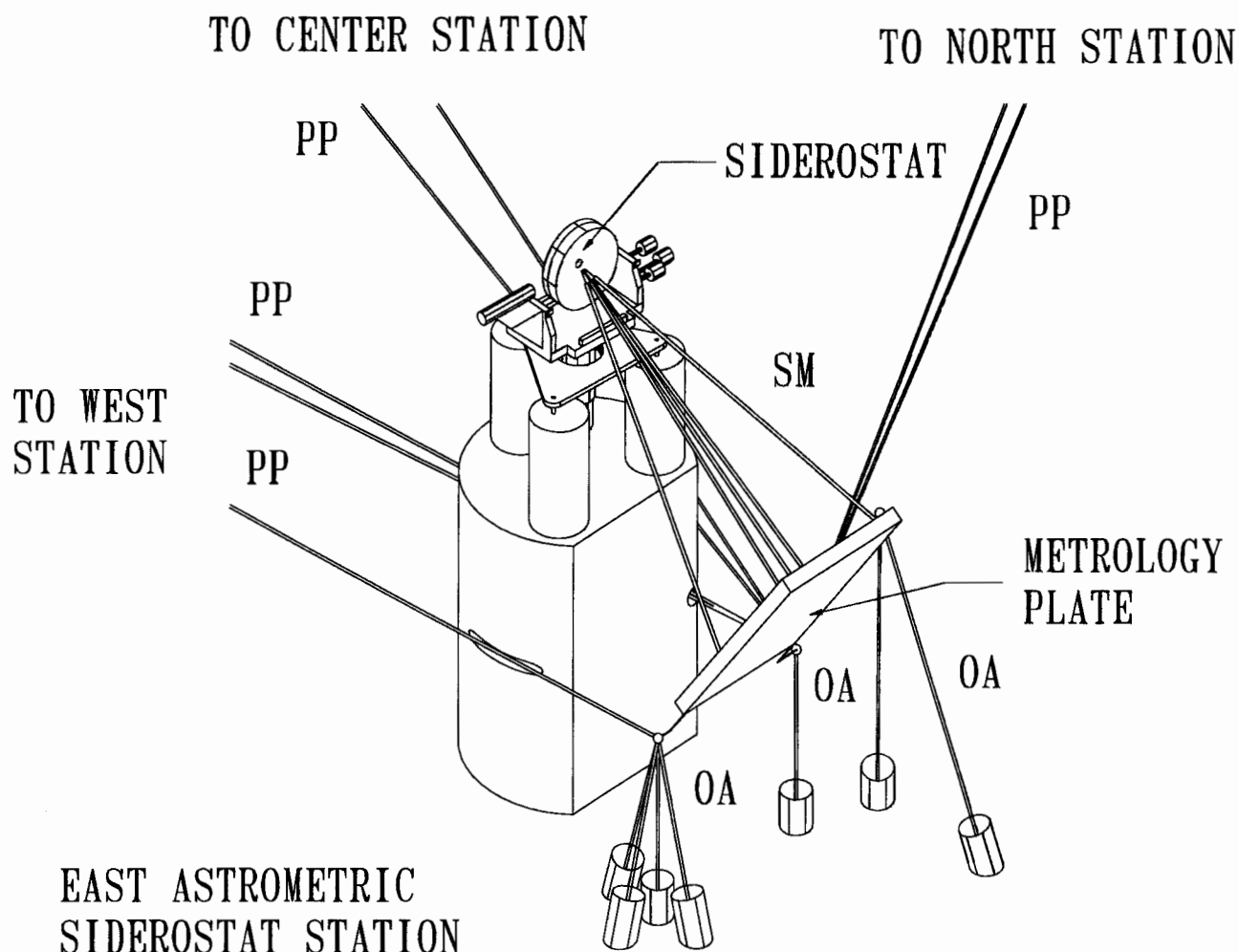
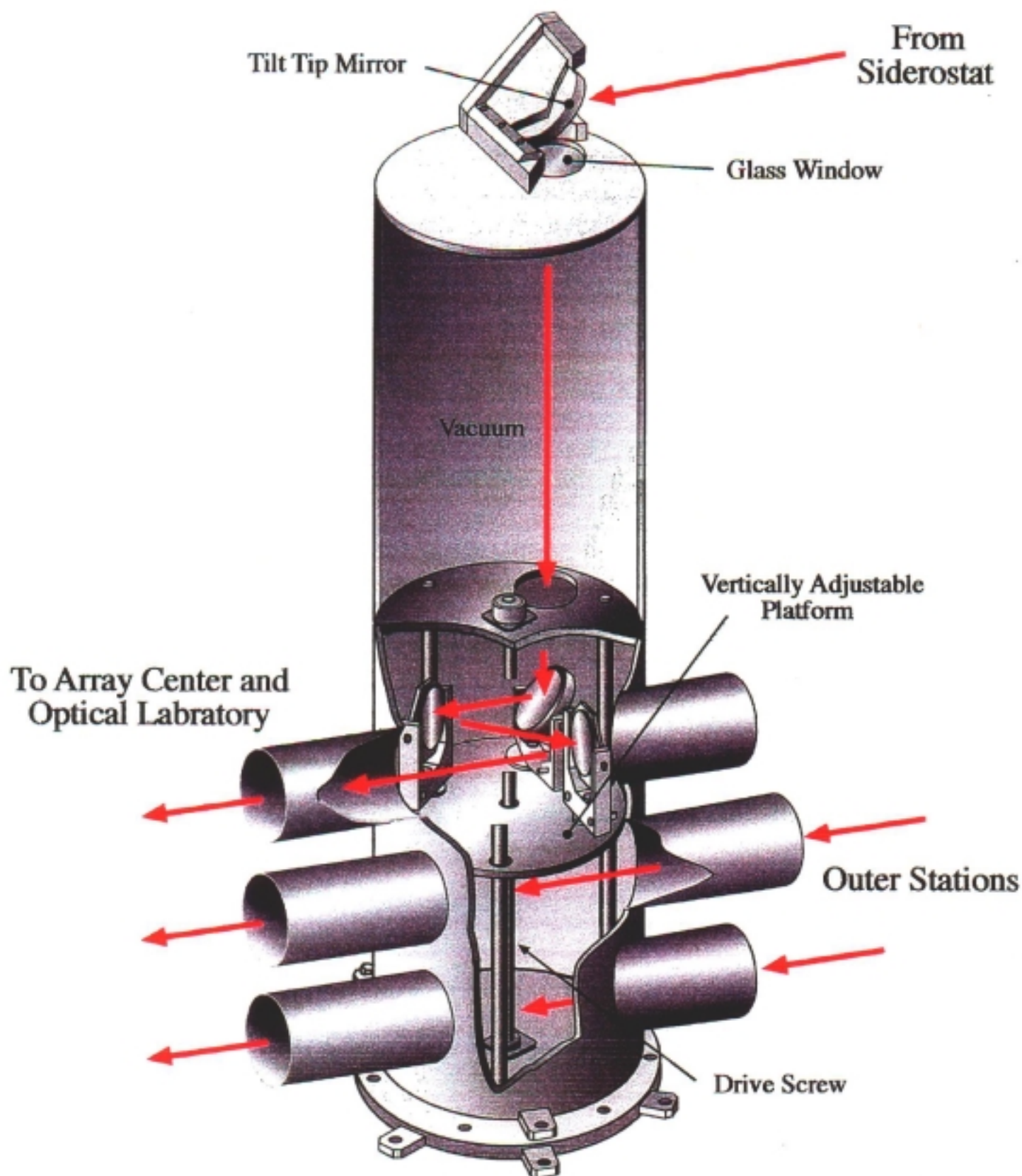


**Figure 6.** The baseline metrology system of the NPOI consists of 60 laser interferometers configured (in three subsystems) to monitor changes in the locations of the siderostats, in three dimensions, with respect to the local bedrock. This elevation view of the east astrometric siderostat station shows parts of the three metrology subsystems: the siderostat metrology (SM; five beams), which monitors the distance from the metrology plate to the siderostat pivot point; the optical anchor metrology (OA; seven beams), which monitors the motion of the metrology plate with respect to bedrock 7 m below the surface; and the pier-to-pier metrology (PP; seven beams), which monitors the horizontal motions of the metrology plates with respect to one another.

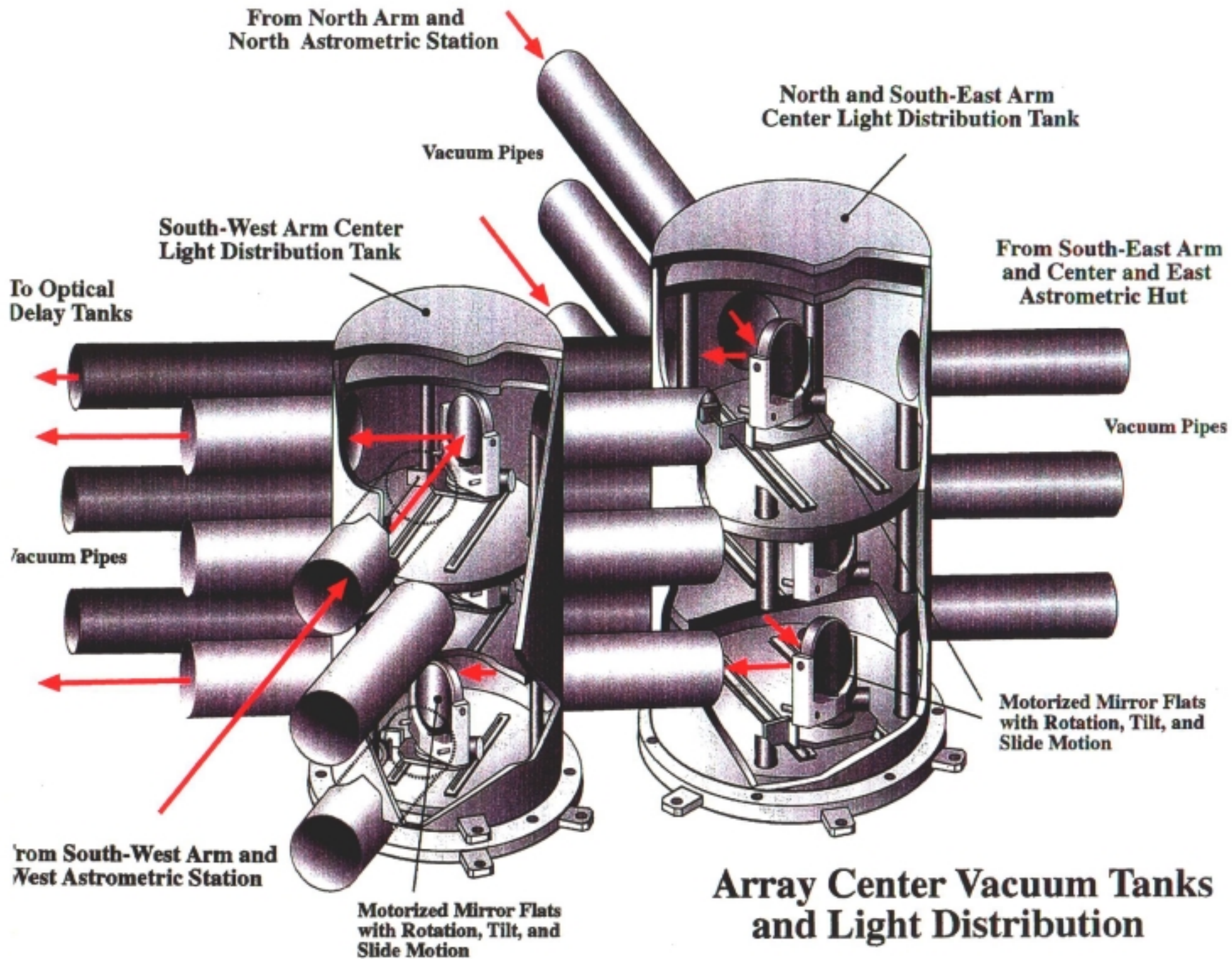
## Vacuum Feed System:

- Makes wideband observations possible by avoiding large air path mismatch within the interferometer (large longitudinal dispersion mismatches) & turbulence
- 12 cm maximum beam size (8" = 20 cm mirror @ 45° incidence)
- 3 pipes/arm  $\Rightarrow$  up to 3 siderostats/arm  
(reconfigurable at each station & array center)
- 6 pipes from array center to lab  $\Rightarrow$  use up to 6 siderostats simultaneously
- inexpensive Neoprene joints (pumped to <10 mT, remains <100 mT ~ 1wk)
- 18 reflections, all overcoated silver, before reaching beam combiner
- Reflections same on each arm same, except for permutations in a horizontal plane):
  - $\Rightarrow$  no differential pupil rotation
  - $\Rightarrow$  polarization dependent phase shifts same on each arm  
( $\leq 1\%$   $V^2$  reduction expected for typical misalignments)

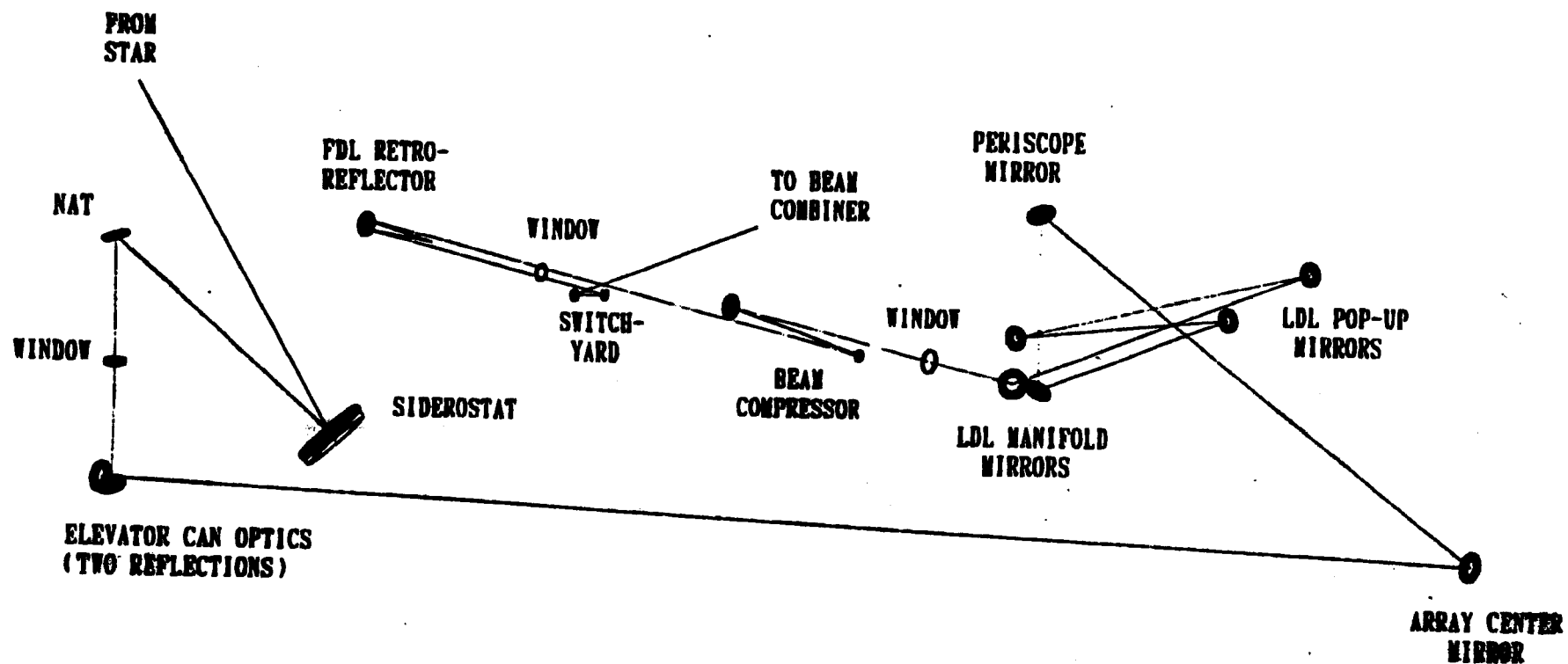


Entrance to Vacuum Light Path  
for  
Southeast Arm





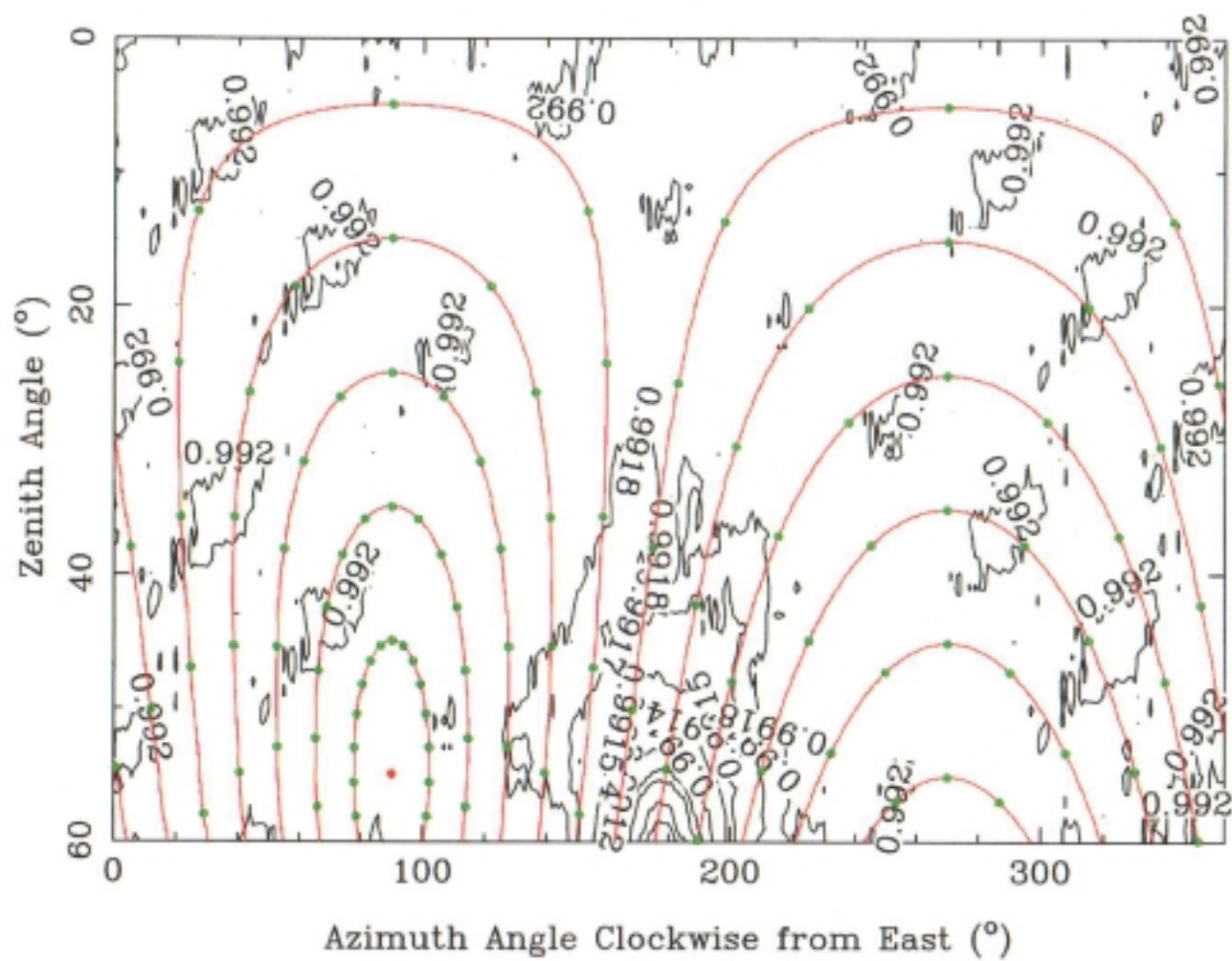




ARMSTRONG et al. (Ref. 1)

## **Baseline Metrology:**

- 100 nm baseline metrology system necessary for 1 mas astrometry on 20 m baseline.
  - NPOI: 55 monitored paths
  - tie baseline to local bedrock  $\Rightarrow$  absolute declinations
- Subsystems:
  - reference table to siderostat metrology
  - optical anchors
  - pier to pier

Instrumental  $|K|^2$ 

## Delay Lines:

- vacuum delay lines make accurate wide-angle astrometry possible:
  - measurement in vacuum  $\Rightarrow$  atmospheric refraction does not affect delays
- also allows wide bandpass:
  - $\Rightarrow$  *astrometry*: allows correction of delay fluctuations by exploiting significant non-linearity of  $(n-1)$  of air at visible wavelengths
  - $\Rightarrow$  *imaging*: large number of simultaneous spatial frequency measurements
- division into LDL and FDL avoids need for 400 m lengths on systems modulating/tracking fringes
- **LDL**: introduces delay in 29 m increments (b/w scans only)
  - Each station contains 2 mirrors on motorized platforms plus mirror tip-tilt
  - Rapid reconfiguration & realignment using CCD camera & movable LED targets

DELAY MATRIX FOR SINGLE LONG DELAY LINE  
DIMENSIONS IN METERS

	A1	A2	A3	A4	A5	A6
B1	0.0	29.2	87.6	146.0	204.5	233.7
B2	29.2	58.4	116.8	175.3	233.7	262.9
B3	87.6	116.8	175.3	233.7	292.1	321.3
B4	146.0	175.3	233.7	292.1	350.5	379.7
B5	204.5	233.7	292.1	350.5	408.9	438.2
B6	233.7	262.9	321.3	379.7	438.2	467.4

VALUES IN RED DENOTE LDL MIRROR  
COMBINATIONS USED

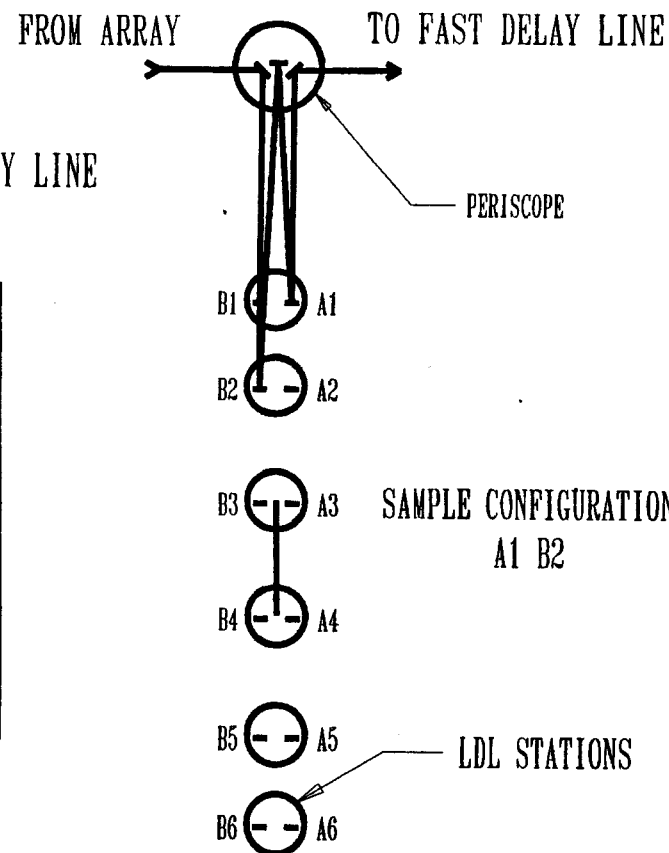
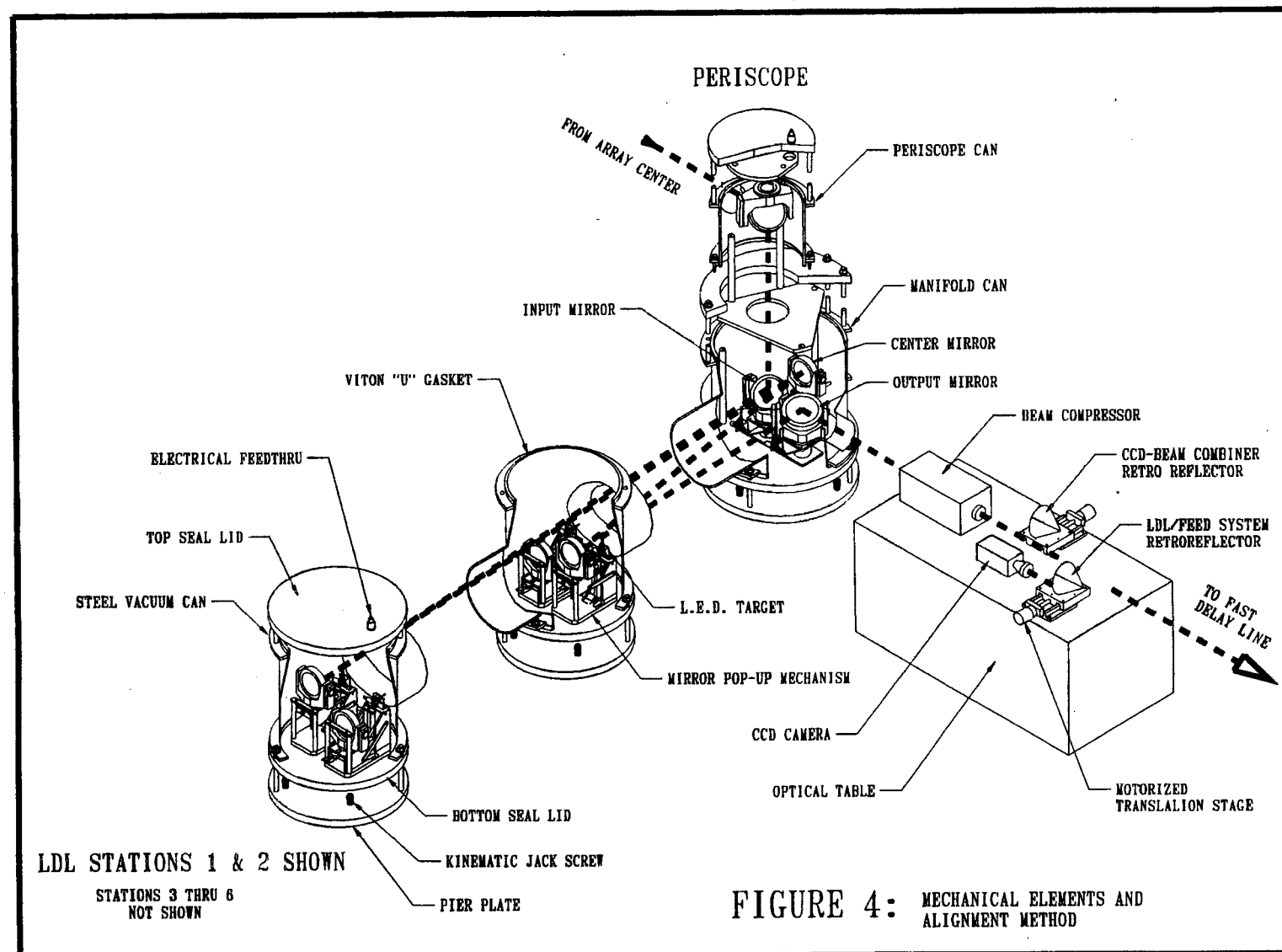


FIGURE 3: DELAY IN LIGHT PATH FOR VARIOUS MIRROR COMBINATIONS



- FDL: continuously variable delay (up to 35m)

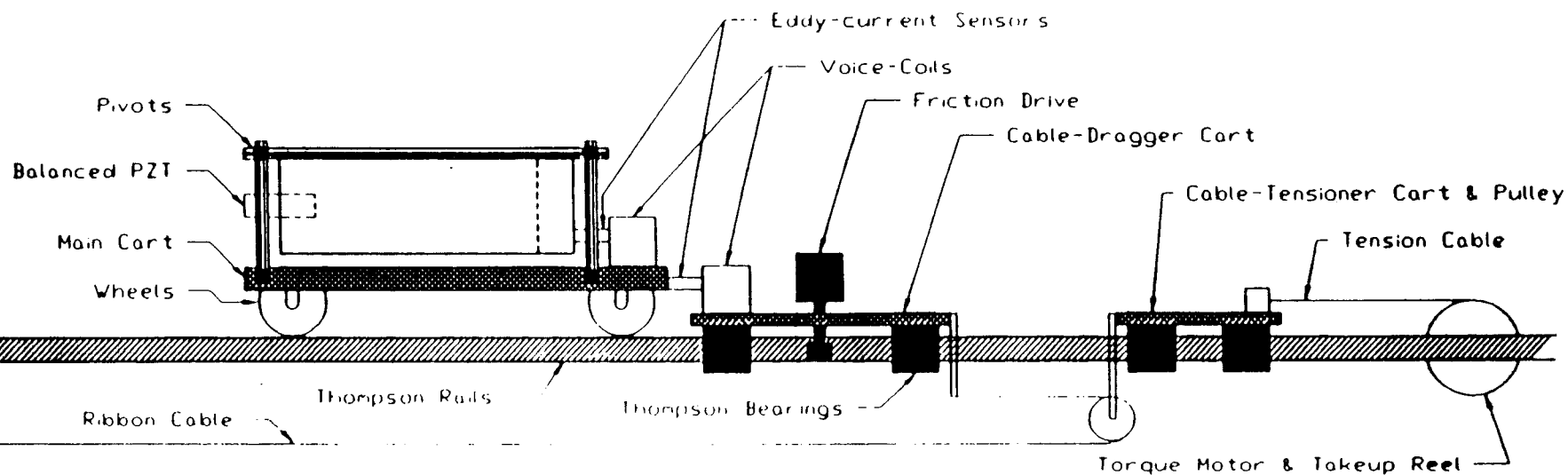
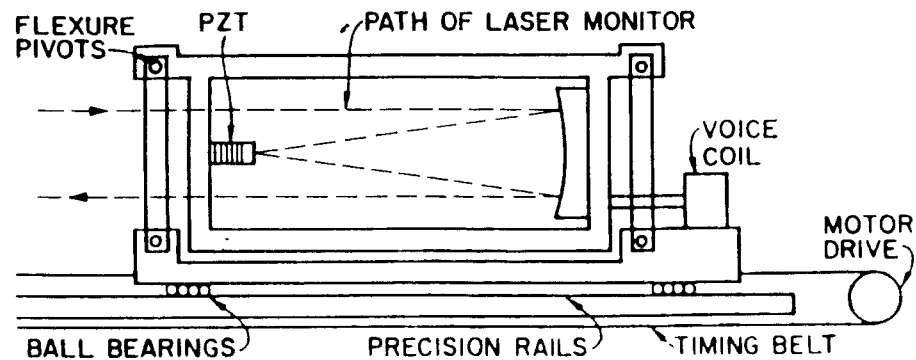
$\Rightarrow$  <sup>track</sup> sidereal delay variation, fringe motion due to atmosphere & <sub>previous</sub>  $\lambda$  delay modulation

- Modified Mark III design, prototype dev at JPL

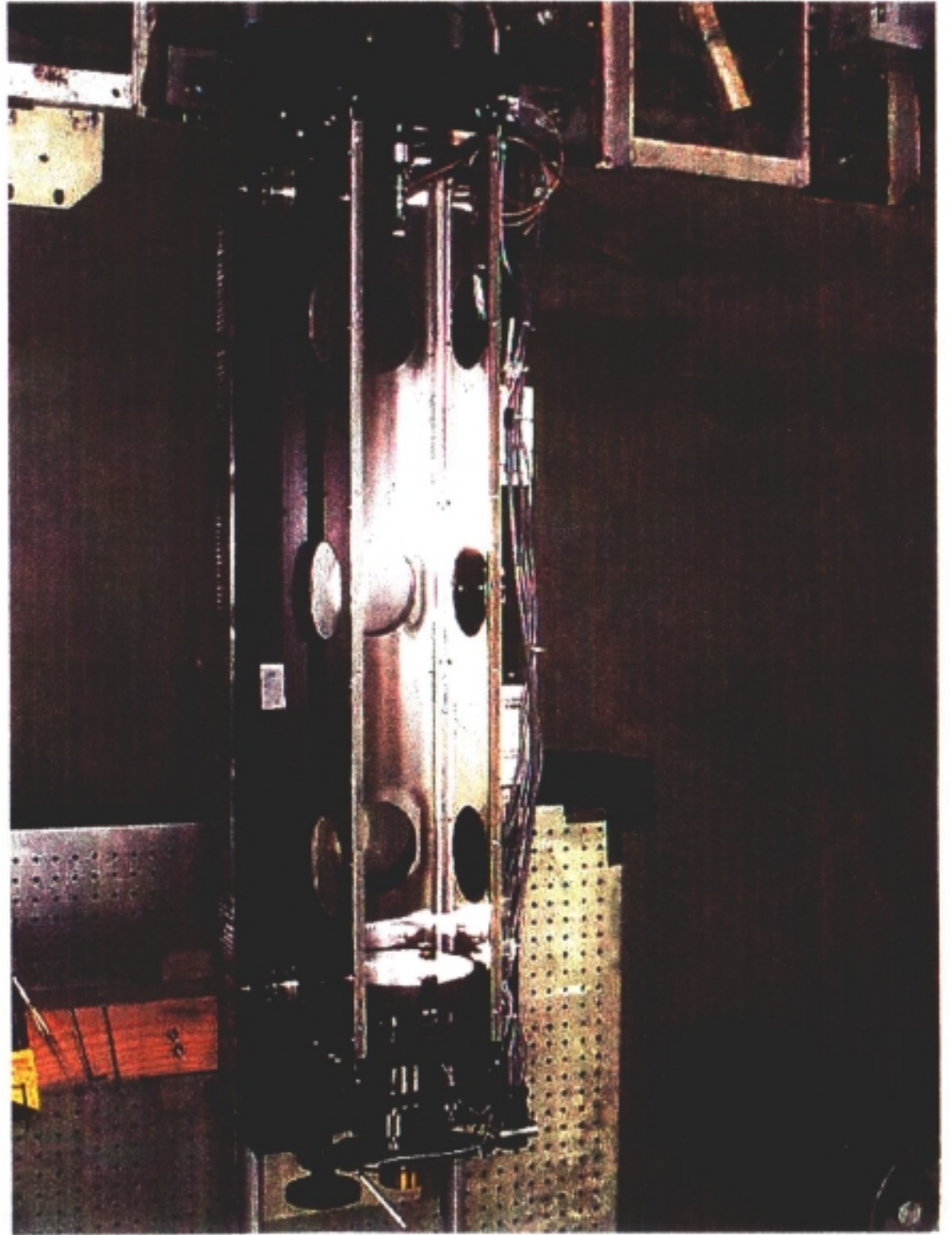
- three level servo:

- 1) stepper motor (on separate cart magnetically linked to main cart)
- 2) voice coil to position optics cage relative to cart base
- 3) piezo under secondary mirror

- corrections generated from position of central starlight interference fringe
- FDLs track fringe motion up to 50 Hz with  $\leq 20$  nm rms noise at speeds up to 2 m/s
- Position measured by laser metrology
- 2<sup>nd</sup> piezo on secondary for delay modulation

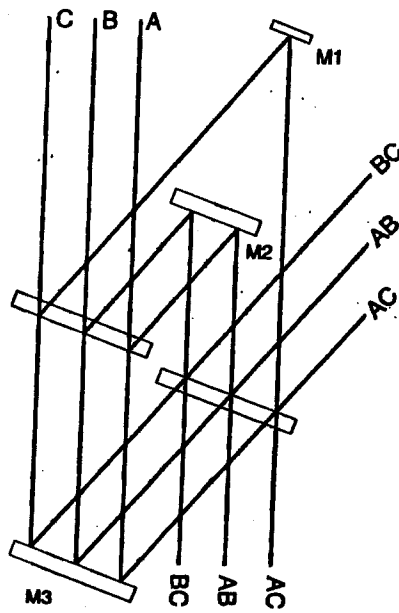




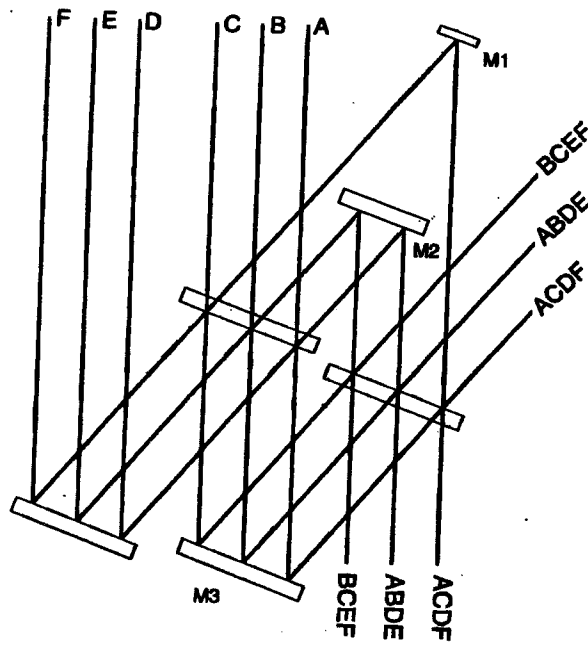


## Beam Combination:

- 3-way beam combiner:
  - pair-wise combination of 3 input beams
  - thermal drift will affect closure phases (non-common beam paths), **but**
  - mechanical/thermal stability keep closure phase drifts of  $2^\circ/\text{hr}$ 
    - $\Rightarrow$  allows calibration with lab or point stellar source
  - each combiner output to spectrometer
    - $\Rightarrow$  each spectrum imaged on linear array of  $400\mu\text{m}$  lenslets bonded to fibers that pass light to APDs



(a)



(b)

- 6-way beam combiner:

- *hybrid* of pair-wise and all-in-one combination

- compromise b/w sensitivity and complexity

(all-in-one combiner more sensitive, but more difficult to build)

- each output is combination of 4 beams (6 baselines)

## Fringe Detection:

- 3-way beam combiner (one baseline/output):

1) 500Hz triangle wave modulation of  $1\lambda$  (opposite phases) on 2 of 3 delay lines

$\Rightarrow$  modulation of delays on baselines of  $1\lambda$  or  $2\lambda$  amplitude

2) detect intensities in each spectral channel synchronously w/delay modulations (8 bins/stroke, widths adjusted w/ wavelength)

$\Rightarrow$  results in 2-D array of photon counts data:  $I_{ij}(x, m)$ ,  
(where  $x$  = wave number,  $m$  = bin number)

3) 2-D FT of this array, at modulation frequency

$\Rightarrow$  peaks in transform yield delay error signal to control FDL

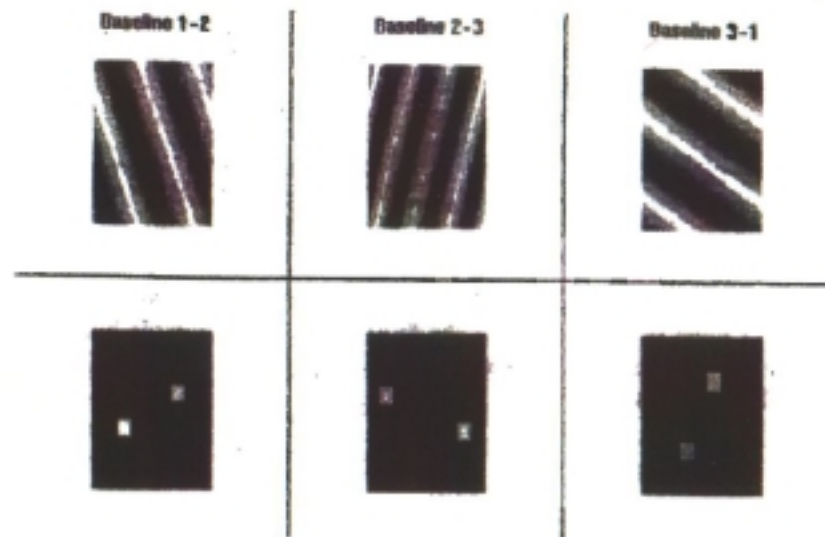


**Figure 1.** The top three panels show simulated data frames (photon counts at each modulation bin vs. wavenumber) for three baselines. The bottom panels show the 2-D Fourier transforms of the upper panels.

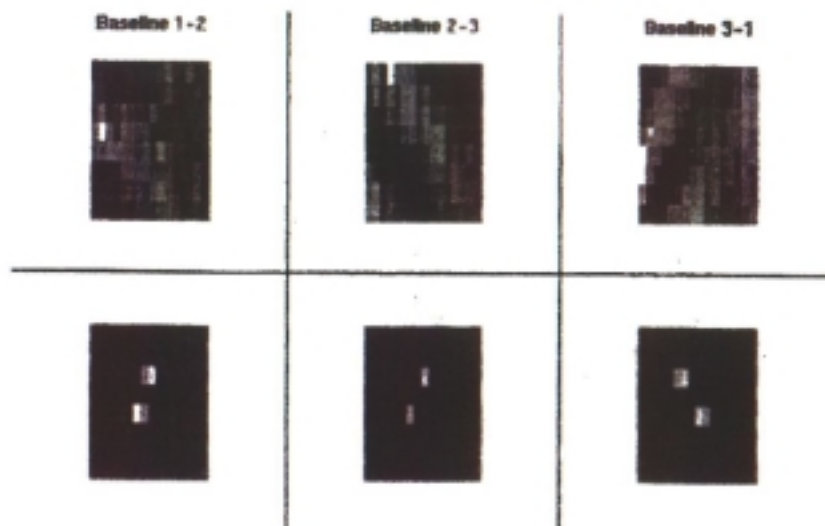


**Figure 2.** The top three panels show real data frames (photon counts at each modulation bin vs. wavenumber) for three baselines. The bottom panels show the 2-D Fourier transforms of the upper panels.

*BENSON (Ref. 2)*

4) photon count arrays saved for off-line science analysis:

- recompute real (X) and imaginary (Y) of complex visibility at each wavelength channel from bins counts ( $B_j$ ,  $j = 0, \dots, 7$ ):

$$X = \Re(V) = \sum_{j=0}^{n-1} B_j \cos\left(\frac{2\pi jk}{n}\right) \Bigg|_{k=1} = (B_0 - B_4) + (B_1 - B_3 - B_5 + B_7)/\sqrt{2},$$
$$Y = \Im(V) = \sum_{j=0}^{n-1} B_j \sin\left(\frac{2\pi jk}{n}\right) \Bigg|_{k=1} = (B_2 - B_6) + (B_1 + B_3 - B_5 - B_7)/\sqrt{2}.$$

( $n = 8$  bins,  $k = 1$  fringe/stroke)

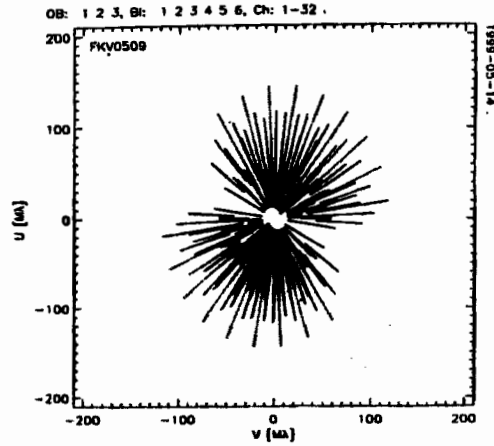
- then  $V^2$  is computed as:

$$V^2 = 4 \left[ \frac{\pi/n}{\sin(\pi/n)} \right]^2 \frac{\langle X^2 + Y^2 - Z^2 \rangle}{\langle N - D \rangle^2},$$

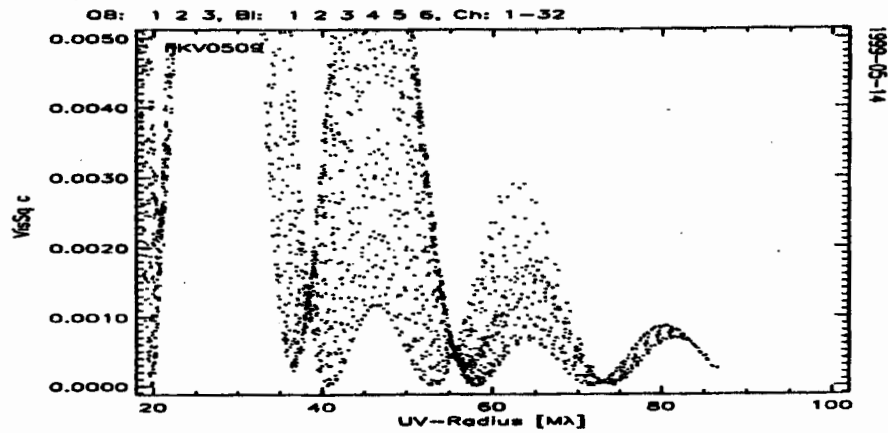
( $N$  = sum photons in 8 bins,  $D$  = background,  $Z^2 = N$  for Poisson statistics)

- 6-way :
  - 4 beams  $\Rightarrow$  6 baselines per output
  - therefore each output must be demodulated at 6 frequencies (max  $8\lambda$  modulation)
  - outputs yield visibility measurements on all 15 possible baselines (3 twice)
  - all 10 independent closure phases (3/output + 1 calc. from all three outputs)
- with large bandwidth & baseline bootstrapping, images  $\geq 10$  resolution elements across disks of nearby late-type stars possible

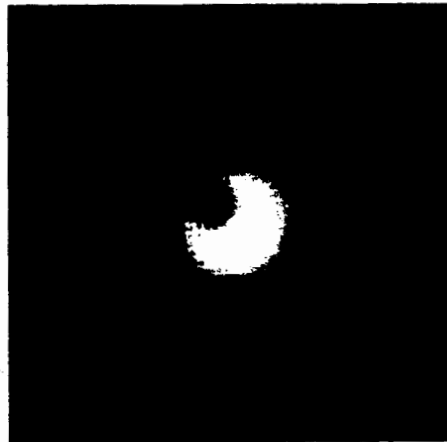




(a)



(b)



(c)

Figure 15.6: Simulation of a 12-mas limb-darkened star with a spot imaged with a six-element array in 32 spectral channels. (a)  $(u, v)$  coverage. (b)  $V^2$  vs.  $\sqrt{u^2 + v^2}$  beyond the first null, before noise addition. (c) Image restored with a maximum-entropy routine.

## References:

- 1) Armstrong *et al.* 1998, ApJ, 496, 550.
- 2) Benson *et al.* 1998, Proc. SPIE, Vol. 3350, p. 493.
- 3) Clark III, J.H. *et al.* 1998, Proc. SPIE, Vol. 3350, p. 497.
- 4) Mozurkewich, D. 1999, in *Principles of Long Baseline Stellar Interferometry*, JPL Pub. 00-009, p. 231.
- 5) Armstrong, J.T. 1999, in *Principles of Long Baseline Stellar Interferometry*, JPL Pub. 00-009, p. 257.